ISSN 0006-2979, Biochemistry (Moscow), 2009, Vol. 74, No. 8, pp. 846-854. © Pleiades Publishing, Ltd., 2009.
Published in Russian in Biokhimiya, 2009, Vol. 74, No. 8, pp. 1042-1051.
Originally published in Biochemistry (Moscow) On-Line Papers in Press, as Manuscript BM09-012, June 28, 2009.

Femtosecond Phase of Charge Separation in Reaction Centers of *Chloroflexus aurantiacus*

A. G. Yakovlev[1]*, T. A. Shkuropatova[2], L. G. Vasilieva[3], A. Ya. Shkuropatov[3], and V. A. Shuvalov[1,3]

[1]*Department of Photobiophysics, Belozersky Institute of Physico-Chemical Biology, Lomonosov Moscow State University, 119991 Moscow, Russia; fax: (495) 939-3181; E-mail: yakov@genebee.msu.su*
[2]*Department of Biophysics, Huygens Laboratory, Leiden University, P. O. Box 9504, 2300 RA Leiden, The Netherlands*
[3]*Institute of Basic Biological Problems, Russian Academy of Sciences, 142290 Pushchino, Moscow Region, Russia; fax: (496) 779-0532; E-mail: shuvalov@issp.serpukhov.su*

Received January 14, 2009
Revision received February 9, 2009

Abstract—Difference absorption spectroscopy with temporal resolution of ~20 fsec was used to study the primary phase of charge separation in isolated reaction centers (RCs) of *Chloroflexus aurantiacus* at 90 K. An ensemble of difference (light-minus-dark) absorption spectra in the 730-795 nm region measured at –0.1 to 4 psec delays relative to the excitation pulse was analyzed. Comparison with analogous data for RCs of HM182L mutant of *Rhodobacter sphaeroides* having the same pigment composition identified the 785 nm absorption band as the band of bacteriopheophytin Φ_B in the B-branch. By study the bleaching of this absorption band due to formation of Φ_B^-, it was found that a coherent electron transfer from P* to the B-branch occurs with a very small delay of 10-20 fsec after excitation of dimer bacteriochlorophyll P. Only at 120 fsec delay electron transfer from P* to the A-branch occurs with the formation of bacteriochlorophyll anion B_A^- absorption band at 1028 nm and the appearance of P* stimulated emission at 940 nm, as also occurs in native RCs of *Rb. sphaeroides*. It is concluded that a nuclear wave packet motion on the potential energy surface of P* after a 20-fsec light pulse excitation leads to the coherent formation of the $P^+\Phi_B^-$ and $P^+B_A^-$ states.

DOI: 10.1134/S0006297909080057

Key words: photosynthesis, charge separation, reaction center, wave packet, electron transfer

The bacterial reaction center (RC) of photosynthesis is a pigment–protein complex responsible for transformation of light energy into the energy of chemical bonds via a series of fast electron transfer reactions. The three-dimensional structure of purple bacteria *Rhodopseudomonas* (*Blastochloris*) *viridis* and *Rhodobacter sphaeroides* RC crystals is known [1, 2]. The RC of *Rb. sphaeroides* consists of three protein subunits (L, M, and H) and several cofactors noncovalently bound to the transmembrane parts of these subunits. These cofactors form two space-symmetrical branches (A and B) consisting of primary electron donor, dimer bacteriochlorophyll (BChl) P, monomeric BChl (B_A and B_B), bacteriopheophytin (BPheo) (H_A and H_B), and quinone (Q_A and Q_B). In purple bacteria, charge separation occurs only in the A-branch, both at room and at low temperature. Upon photoexcitation of P, an electron transits from the lowest excited singlet state P* to H_A with a time constant ~3 psec at room and ~1.5 psec at low temperature in accordance with a formation of the charge separated state $P^+H_A^-$. Then the electron transits from H_A^- to Q_A with a time constant ~200 psec at room and ~100 psec at low temperature, forming the $P^+Q_A^-$ state. The overall quantum yield of the charge separation process is close to unity at all temperatures at which it has been measured (see reviews in [3-5]).

Like RCs of purple bacteria, the RC of the thermophilic green bacterium *Chloroflexus aurantiacus* consists of BChl dimer as the primary electron donor, BPheo as an intermediate electron acceptor, and two menaquinone molecules Q_A and Q_B [6-13]. The three dimensional structure of this RC is not yet known [14]. Comparison of the polypeptide structure, spectroscopic

Abbreviations: ΔA, absorption difference (light minus dark); BChl, bacteriochlorophyll; B_A and B_B, monomeric BChl in A- and B-branch, correspondingly; BPheo, bacteriopheophytin; H_A and H_B, BPheo in A- and B-branch, correspondingly; Φ_B, BPheo which substitutes BChl B_B; P, primary electron donor, dimer of BChl; Q_A and Q_B, quinone in A- and B-branch, correspondingly; RC, reaction center.

* To whom correspondence should be addressed.

data, and calculations based on exciton theory shows that the cofactors from *C. aurantiacus* RC form two pigment branches like in the *Rb. sphaeroides* RC [15-22]. It was found that the electron transfer rate to H_A in *C. aurantiacus* RC is less than that for *Rb. sphaeroides* [23, 24]. At 296 K, the decay of P* occurs with a time constant of 7 psec, but at 10 K two components with time constants of 2 and 24 psec are distinguished in the P* decay. The quantum yield of primary charge separation is close to 1 at 280 K [25] and at room temperature [26]. It is proposed that the accessory molecule of BChl B_A participates in electron transfer from P* to H_A as a mediator [26, 27]. The further electron transfer from H_A^- to the primary quinone Q_A with the formation of the $P^+Q_A^-$ state occurs in *C. aurantiacus* RC with the time constant of ~320 psec at 280 K [9].

Despite similarity with bacterial RCs in chromophores arrangement and photochemistry, the RC of *C. aurantiacus* has some significant differences in protein and cofactor composition (reviewed in [6]). Some amino acid residues from RCs of purple bacteria are absent in *C. aurantiacus* RC. For example, in *C. aurantiacus* RC Leu is present instead of Tyr M210, which might explain a slowing of primary charge separation reaction. Note that the B-branch of *C. aurantiacus* RC contains two molecules of BPheo, Φ_B and H_B, and Φ_B is in the B_B site [10, 28]. In purple bacteria the free energy level of the $P^+B_B^-$ state lies 240 meV higher than that of P*, and the $P^+B_A^-$ level is slightly below P* [29, 30]. It is accepted that this difference of free energy levels is an important factor determining absence of functional activity of the B-branch [29, 30]. The midpoint potential of the BPheo/BPheo$^-$ redox couple *in vitro* is 230-300 meV more positive than that for the BChl/BChl$^-$ couple [31, 32], which facilitates the reduction of BPheo *a* Φ_B in comparison with BChl *a* B_B. On the other hand, the midpoint potential of the P/P^+ couple in *C. aurantiacus* RC is 70-90 meV lower than in *Rb. sphaeroides* RC [7, 20]. So, the energy level of $P^+\Phi_B^-$ in *C. aurantiacus* RC might be close or even below the P* level, which might make possible electron transfer to the B-branch. Electron transfer in B-branch is clearly observed in RC of HM182L mutant of *Rb. sphaeroides*, in which a BPheo Φ_B molecule is placed in the B_B site by changing the histidine ligand of B_B at position M182 to a leucine [33, 34]. The quantum yield of charge separation with the formation of $P^+\Phi_B^-$ state is 35% at room [33] and 12% at low temperatures [34] in this mutant. In [35] it was concluded that low-temperature kinetics of fluorescence in *C. aurantiacus* RC with reduced Q_A can be explained by the possibility of a fast reversible electron transfer between P* and the BPheo in the B-branch. However, the results of difference absorption spectroscopy in the Q_x band of BPheo molecules and close to 1 quantum yield of primary charge separation in *C. aurantiacus* RC indicate electron transfer along the A-branch only [25, 26, 36].

Femtosecond optical spectroscopy can be used to reveal nuclear coherent dynamics accompanying electron transfer reactions. In [37-40] oscillations in the kinetics of stimulated emission of P* excited by femtosecond light was found in RCs of purple bacteria. Analogous oscillations have been found in the kinetics of spontaneous fluorescence [41]. It was shown that the origin of these oscillations is formation and coherent motion of the nuclear wave packet on the potential energy surface of P* [38, 39, 42]. Coherent oscillations have been found in the kinetics of the charge separated states $P^+B_A^-$ and $P^+H_A^-$ also [43-48]. Modulation of the population of the $P^+B_A^-$ state was found in *Rb. sphaeroides* R-26 RC by measuring the absorption kinetics at 1020 nm characteristic for the formation of radical anion B_A^- [5, 32, 44-47]. Oscillating motion of the wave packet on the surface of P* near the long-wavelength side (935 nm) is accompanied by reversible electron transfer from P* to B_A. This leads to a modulation of the B_A^- absorption band at 1020 nm with a period of about 260 fsec [44-47]. Coherent oscillations of the population of the $P^+H_A^-$ state were revealed in *Rb. sphaeroides* RC [46-48]. Femtosecond oscillations in the kinetics of stimulated emission of P* at 945 nm and of B_A^- absorption at 1028 nm were found in *C. aurantiacus* RC at 90 K [49]. The kinetics at 1028 nm reflect stabilization of the $P^+B_A^-$ state with a characteristic time of ~5 psec and electron transfer to H_A within ~1 psec.

In the present work, the initial femtosecond phase of charge separation was studied in *C. aurantiacus* RC by coherent absorption spectroscopy with ~20-fsec resolution at 90 K. The possibility of electron transfer in the B-branch with participation of a Φ_B molecule was examined. We systematically compared our results with earlier results for mutant HM182L *Rb. sphaeroides* RC [50] having the same pigment composition (3 BChl : 3 BPheo) and clear photochemistry of the B-branch [33, 34]. The possibility of coupling between electron transfer in the B-branch and nuclear wave packet motion was studied also. The results indicate electron transfer from P* to Φ_B during the earliest stages of the charge separation process in *C. aurantiacus* RC. It was found that in both types of RCs coherent electron transfer in the B-branch starts immediately after excitation of P when the wave packet emits at 900 nm and the $P^+B_A^-$ state is not yet formed. This state is formed 120 fsec after excitation when the wave packet reaches the opposite side of the P* potential surface and begins to emit at 940 nm.

MATERIALS AND METHODS

Chloroflexus aurantiacus RC was prepared according procedures described in [20, 28] with minor changes. Cells were sonicated in 50 mM Tris-HCl buffer (pH 8.5). After removal of unbroken cells and debris, membranes were isolated by centrifugation at 100,000*g*. Then mem-

branes (A_{865} = 15 cm^{-1}) were incubated with 1% lauryldimethylaminoxide (LDAO) in 50 mM Tris-HCl buffer (pH 8.5) in the presence of 50 mM NaCl at 37°C for 1 h and centrifuged at 100,000*g* for 2.5 h. To prevent partial destructive oxidation of the RC, 10 mM sodium dithionite was added to the incubation mixture. Then the RC was purified by repeated anion-exchange chromatography on DEAE cellulose DE52 columns and eluted with 50 mM Tris-HCl, pH 8.5/0.1% LDAO/60 mM NaCl buffer. Before measurements, the LDAO detergent was exchanged for Triton X-100 in the buffer solution of RC by repeated cycles of diluting with 50 mM Tris-HCl, pH 8.5/0.05% Triton X-100 and re-concentrating on a membrane under pressure in an argon atmosphere. By this procedure, the samples were desalted. Measurements at 90 K were performed on samples containing 65% (v/v) glycerol. The absorption of the RCs samples at 860 nm was 0.5 in a 1-mm optical path cuvette at room temperature. To keep the RC in the state $PB_AH_AQ_A^-$, 5 mM sodium dithionite was added to the samples. Absorption spectra of non-excited samples were measured on a Shimadzu UV-1601 PC spectrophotometer.

Difference (light-minus-dark) absorption spectra with femtosecond resolution were measured using a laser spectrometer described in [44]. The operating frequency of the spectrometer was 15 Hz. The duration of pump and probe pulse was about 20 fsec. The pump wavelength was 870 nm. The temporal delay between pump and probe pulses was set with an accuracy of 1 fsec. Temporal dispersion in the 720-790 and 940-1060 nm ranges was less than 30 fsec as determined by the bleaching spectra of a ZS-10 glass filter (LOMO, Russia). The difference absorption spectra obtained by averaging 7000-10,000 measurements at each delay were the initial data. The minimal value of measuring ΔA was (1-3)·10^{-5} optical density units. The kinetics of absorbance changes ΔA were plotted for the center wavelengths of the characteristic bands in the difference absorption spectra after subtraction of broadband background [47]. For the extraction of oscillatory parts from the kinetics, a polynomial approximation followed by subtraction of a non-oscillatory component was applied. This approach is more acceptable for non-adiabatic processes of charge separation under femtosecond excitation than a standard exponential approximation [47]. The oscillations of the kinetics were subjected to Fourier analyses for obtaining the oscillation frequency data.

RESULTS AND DISCUSSION

Figure 1 shows the absorption spectra and their second derivatives of non-excited RC of *C. aurantiacus* (thick lines) at room temperature. For comparison the analogous spectra are shown by thin lines for mutant HM182L *Rb. sphaeroides* RC normalized to the spectrum

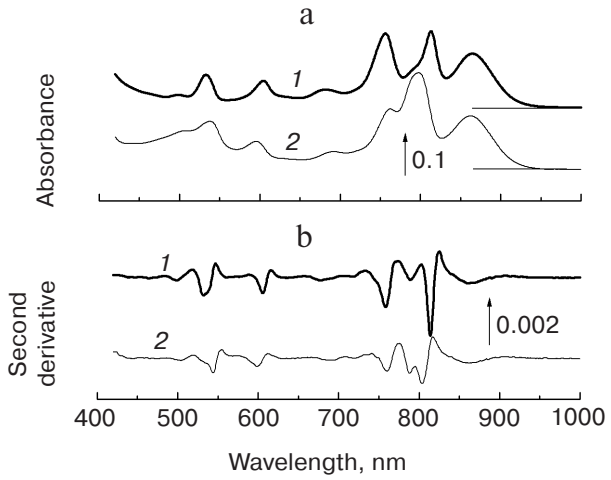

Fig. 1. Absorption spectra (a) and their second derivatives (b) of *C. aurantiacus* RC (*1*) and *Rb. sphaeroides* mutant HM182L RC (*2*) [50] at room temperature. Spectra are normalized at the maximum of the 865-nm band.

of *C. aurantiacus* at the maximum of the long-wavelength band at 865 nm (data are taken from [50]). The spectra of both RC types are identical to those obtained earlier [8, 10, 11, 23, 28, 33, 51, 52]. In the region of Q_y transitions, both RC types have an absorption band at 865 nm corresponding to the exciton transition with low energy in the dimer BChl, which is the primary electron donor P. In the spectrum of *C. aurantiacus* RC the band at 813 nm is mainly ascribed to the accessory BChl (B_A), and the slightly asymmetric band at 756 nm is ascribed to BPheo molecules. Revealing of absorption bands of the Φ_B molecule as a nearest neighbor of P among the cofactors of the B-branch of *C. aurantiacus* RC is important for study the possibilities of electron transfer in this branch. It is well known that in *C. aurantiacus* RC the absorption at 760 nm is larger than in *Rb. sphaeroides* RC containing only H_A and H_B [10, 28]. Since H_A and H_B molecules of *C. aurantiacus* RC and of *Rb. sphaeroides* RC have a similar extinction coefficients, this means that Φ_B contributes to the absorption at 756 nm in *C. aurantiacus* RC. In RC of the HM182L mutant of *Rb. sphaeroides*, the Φ_B molecule has the Q_y transition at 785 nm (788 nm according to the second derivative, Fig. 1b) overlapping with the BChl B_A transition at 803 nm, which results in the broad absorption band at 797 nm ([33], Fig. 1). A similar relatively weak absorption band at 785 nm is seen in *C. aurantiacus* RC (Fig. 1). A number of authors suppose that this is the high-energy exciton transition band of dimer P [21, 22] with some contribution of the accessory BChl absorption [21]. Note that the 785 nm band is only observed in the RC with modified in comparison with *Rb. sphaeroides* composition of B-branch pigments. The difference between the spectra of RC from *C. aurantiacus* and from HM182L mutant of *Rb. sphaeroides* in the 740-785-nm

region can be explained in two ways. First, most of the Φ_B dipole strength in the HM182L mutant can be at 785 nm. Second, a contribution of charge transfer to the 785-nm transition might be much more considerable in HM182L mutant than in *C. aurantiacus*. On lowering the temperature, the absorption bands of *C. aurantiacus* and HM182L mutant RCs become narrower, and the long-wavelength transition of P shifts to the red to 887 nm at 77 K, while the spectra of the other bands are almost unshifted [18, 19, 23, 28, 34, 53].

In Fig. 2, the difference (light-minus-dark) absorption spectra of *C. aurantiacus* RC measuring with 20-fsec resolution at 90 K are shown in the 735-792-nm region at various temporal delays from the excitation moment at 870 nm. Here and below the zero delay corresponds to half of the maximum of the P absorption band bleaching at 880 nm, which occurs almost at the same moment with P excitation. The analogous spectra for mutant HM182L of *Rb. sphaeroides* at 38-fsec delay taken from [50] is shown for comparison in the inset. Characteristic features of the ΔA spectra of *C. aurantiacus* RC in Fig. 2 are the bleaching with peaks at 748-750 and 785 nm and increasing of ΔA with the peak at 763-765 nm. The spectral positions of these peaks have almost no dependence on delay. These features are observed for the measurements in the whole delay range 0-4 psec including the delays less than 30 fsec. In the absorption band at 755 nm (Fig. 1), a red shift and possibly a pure increase are observed that are reflected in the difference spectra as a decrease at 750 nm and an increase at 765 nm with different amplitudes. This spectral feature is observed at the earliest delay of 13 fsec. In contrast, the ΔA spectra of the HM182L mutant (inset in Fig. 2) contain a blue shift of the 755-nm absorption band and a bleaching at 785 nm [50]. Perhaps the opposite direction of the shifts in the ΔA spectra of the two RC types is due to the contribution of the Φ_B molecule to the transition at 750-760 nm in *C. aurantiacus* RC, while in the HM182L mutant RC only H_A and H_B molecules absorb at 750-760 nm. Nevertheless, the origin of these spectral shifts remains unclear. One can only assume that these shifts are electrochromic and reflect the appearance of the charge near the BPheo molecules in the B-branch in the initial step of charge separation between P_A and P_B under femtosecond excitation of P. Our ΔA spectra of *C. aurantiacus* RC at 30-60 fsec delays are very similar to the analogous spectra of mutant HM182L *Rb. sphaeroides* RC at 190 psec delay that were obtained at cryogenic temperature and reflect the formation of the $P^+\Phi_B^-$ state [34]. This is evidence of the fact that the absorption decrease at 785 and 748 nm in the ΔA spectra of *C. aurantiacus* RC (Fig. 2) in the femtosecond region is a consequence of the bleaching of the Q_y band of the Φ_B molecules caused by photoreduction.

In Fig. 3 the kinetics of ΔA of *C. aurantiacus* RC (upper row), their oscillatory components (middle row), and Fourier spectra of oscillations (lower row) at 748, 763, and 785 nm are shown. The kinetics were plotted on the basis of the absorption spectra in the 730-792 nm region at 0 to 4 psec delays, which are shown in Fig. 2 for some delays. All kinetics contains a fast (less than 50 fsec) absorption change followed by slower change tending to the intermediate steady-state limiting level that reflects the gradual formation of the $P^+H_A^-$ state. The kinetics at 748 and 785 nm show a monotonous increase in ΔA signal, while the 763-nm kinetics mostly consist of monotonous decrease. All three kinetics contain oscillations damping almost completely within ~1 psec. The oscillatory part of the kinetics at 785 nm contains ~1.5 modulation periods with an average frequency ~200 $fsec^{-1}$. The Fourier spectrum of this oscillatory component looks like a band with a ~100 cm^{-1} bandwidth and distinct maximums at 108 and 79 cm^{-1}. The oscillations from the kinetics at 748 nm contain ~3 modulation periods with ~150 $fsec^{-1}$ frequency. In the Fourier spectrum of this oscillation a broad (~70 cm^{-1}) band with maximum at 154 cm^{-1} and narrower band at 73 cm^{-1} dominate. The peaks at 10 cm^{-1} have an artificial origin and deal with a non-symmetrical behavior of the oscillation curves. In the kinetics, oscillations at 763 nm with ~1.5 periods of modulation with ~200 $fsec^{-1}$ frequency are seen on the background of intense high-frequency noise. The corresponding Fourier spectrum is very noisy and contains a band at ~100-150 cm^{-1}. Oscillations with 100-150 cm^{-1} frequencies are observed in the kinetics of P* stimulated emission and in absorption bands of pigments taking part in primary charge separation [5, 49]. Based on these facts, one can assume that the kinetics at 785 and 748 nm

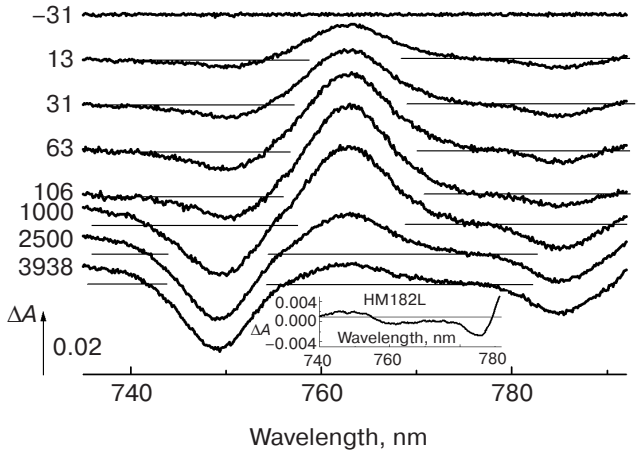

Fig. 2. Difference (light-minus-dark) absorption spectra of *C. aurantiacus* RC in the 730-792-nm region at various temporal delays from light excitation. The RC was excited by 20-fsec pulses at 870 nm at 90 K. A zero delay here and in Figs. 3-5 corresponds to the half of P band maximal bleaching at 880 nm, which occurs simultaneously with the excitation. In the inset the difference absorption spectrum of HM182L mutant of *Rb. sphaeroides* RC is shown measured under the same conditions at 38 fsec delay, taken from [50]. Numbers are the delays in femtoseconds.

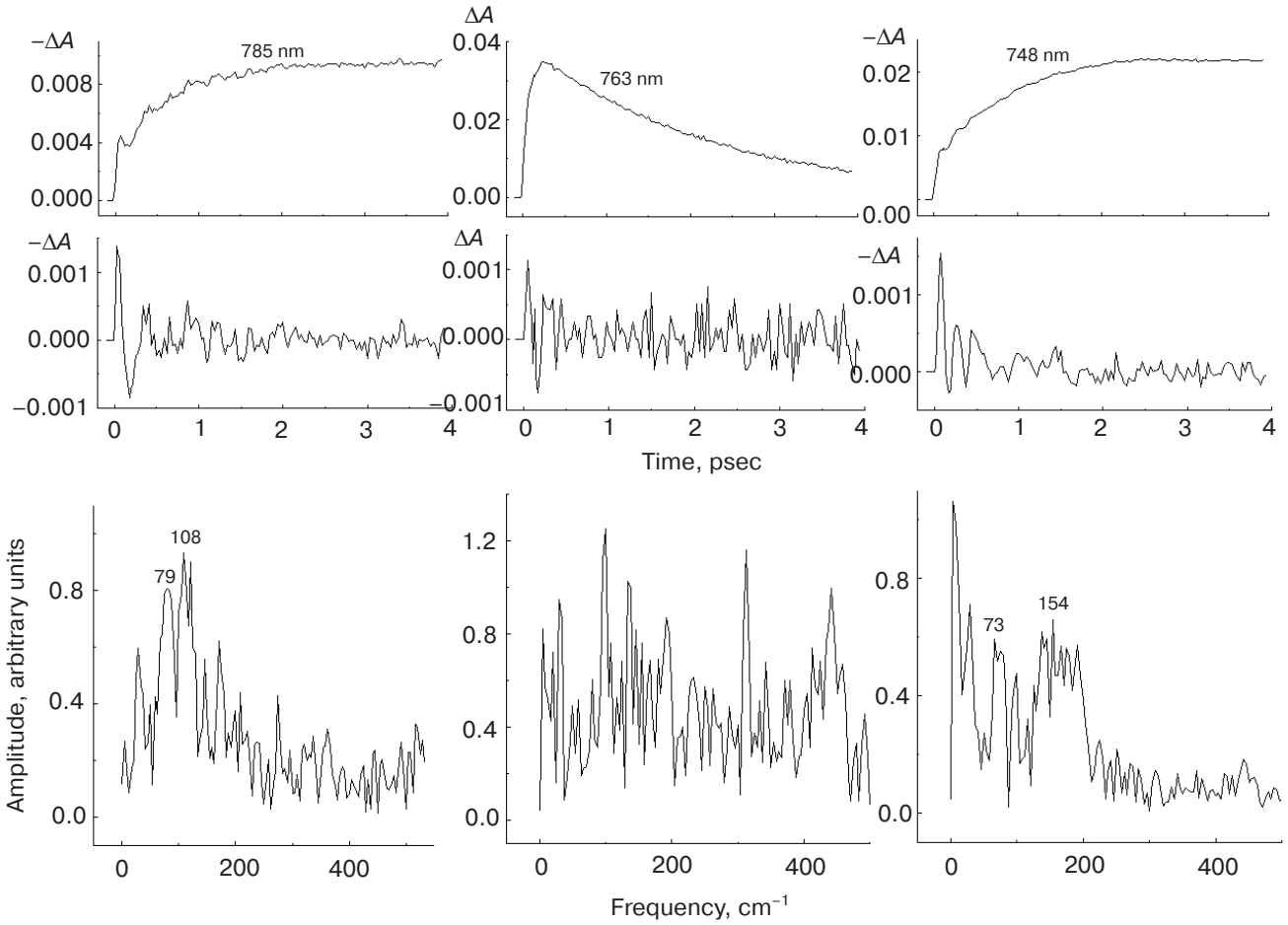

Fig. 3. Kinetics of ΔA of *C. aurantiacus* RC (upper row), their oscillatory components (middle row), and Fourier spectra of the oscillations (lower row) at 748, 763, and 785 nm. The kinetics were plotted on the basis of ΔA spectra in the 730-792 nm region in the delay range of −0.1 to 4 psec. The RC was excited by 20-fsec pulses at 870 nm at 90 K.

reflect a process of electron receiving from P* by the Φ_B molecule.

In Fig. 4 the kinetics (a) and their oscillatory parts (b) at 748 (*1*) and 785 nm (*2*) are presented within a smaller delay region (−100 to 400 fsec). The kinetics at 785 nm for mutant HM182L RC of *Rb. sphaeroides* taken from [50] are also presented (Fig. 4b, curve *3*). The kinetics of *C. aurantiacus* RC at 785 nm are the same as in Fig. 3. The kinetics at 748 nm are the result of subtraction of the ΔA spectrum at 13-fsec delay normalized at 763 nm from the ΔA spectra at other delays in the 735-770 nm region. This subtraction excludes from the ΔA spectra a component associated with the red shift of the *C. aurantiacus* RC absorption band at 755 nm (Fig. 1). The band of the "pure" bleaching at 748 nm is the result of this subtraction. In the inset of Fig. 4a, the result of this subtraction is shown for the 43-fsec delay. The bleaching of the 785-nm band rises at very small delay (~10 fsec) after photoexcitation of P. The bleaching of the 748-nm band rises at slightly longer delay of ~30 fsec. At a later time, oscillations of the kinetics at 748 and 785 nm have almost synchronous behavior reaching a zero level at 100 fsec, negative maximum at 175 fsec, and positive maximum at 250 fsec. The fact that the oscillations of the kinetics at 748 and 785 nm are in phase with each other is consistent with assigning both transitions to the Φ_B molecule, which is reversibly reduced when it receives an electron from P*. Analogous oscillations are observed in the kinetics of HM182L mutant RC of *Rb. sphaeroides* at 785 nm, taken from [50] (Fig. 4b, curve *3*). These oscillations are ~20-fsec delayed from the excitation moment and reach a maximum at ~40 fsec.

In Fig. 5 the ΔA kinetics of *C. aurantiacus* (a) and HM182L mutant of *Rb. sphaeroides* (b) RCs are shown at 940 (*1*) and 1020-1028 nm (*2*) in the −100 to 400-fsec delay region. The characteristic ΔA spectra are shown in the insets for the 990-1050-nm region. The *C. aurantiacus* data are taken from [49], and the HM182L mutant data are taken from [50]. The 940-nm kinetics reflect the long-wavelength region of stimulated emission of P*, and the 1020-1028-nm kinetics reflect the formation of the B_A^- absorption band by the reduction of B_A. The presented

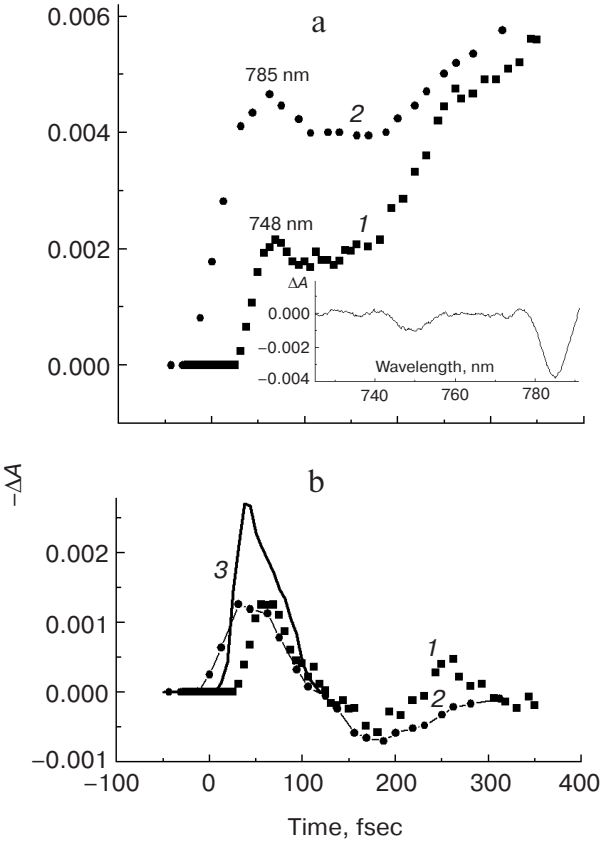

Fig. 4. Kinetics of ΔA of *C. aurantiacus* RC (a) and their oscillatory components (b) at 748 (*1*) and 785 nm (*2*) in the delay range of −100 to 350 fsec, plotted on the basis of ΔA spectra. The kinetics at 748 nm are the result of subtraction of the ΔA spectrum at 13-fsec delay normalized at 763 nm from the ΔA spectra at other delays in the 735-770 nm region. In the inset, the result of this subtraction is shown for the 43-fsec delay. The RC was excited by 20-fsec pulses at 870 nm at 90 K. Curve *3*, kinetics of HM182L mutant RC of *Rb. sphaeroides* at 785 nm [50].

kinetics of both RC types contains oscillations that develop synchronously and have a significant delay of ~110 fsec from the moment of photoexcitation of P. This means that the nuclear wave packet formed by the 20-fsec excitation of P reaches the intercrossing area of P* and $P^+B_A^-$ potential energy surfaces within the first half-period of oscillation at 1028 nm (the period is ~190 fsec) [49]. Together, the data shown in Figs. 2-5 indicate that in *C. aurantiacus* RC an electron is transferred from P* to Φ_B immediately after the nuclear wave packet formation, while the electron transfer to B_A is delayed by 110-fsec, which is enough for the electron to leave the Φ_B molecule. The same picture is observed in HM182L mutant RC of *Rb. sphaeroides* (Fig. 5b). In this RC the Φ_B band bleaching at 785 nm is delayed by only ~25 fsec from the moment of photoexcitation of P (Fig. 4b, curve *3*), while the formation of the B_A^- absorption band at 1020 nm is delayed by 120 fsec. The same delay of the B_A^- absorption band formation is observed in the native RC of *Rb. sphaeroides* [47].

Based on these results, one can plot a simplified scheme of potential energy levels for the non-equilibrium conversion of P* excited state into the charge-separated states in *C. aurantiacus* RC (Fig. 6). The dimer P has a non-uniform distribution of electron density in the P^+ state with a predominate shift of π-electron density to P_A (0.74/0.26) [54]. Thus, the upper orbital of P ground state is mostly an orbital of P_A. The 20-fsec photoexcitation of P creates the nuclear wave packet on the potential energy surface of the lowest exciton state $\sqrt{½}\{|P_A^*P_B> + |P_AP_B^*>\} \equiv |+>$ with emission at 895 nm (electron coupling between P_A and P_B has a negative energy of ~600 cm^{-1}). The formation of the $P_A^{\delta+}P_B^{\delta-}$ state in the P* excited state is possible, though the reorganization energy is too high at this place on the potential surface. Electron transfer from P_A^* to BChl B_B in native *Rb. sphaeroides* RC is forbidden because the LUMO energy level of B_B is higher than of P_A according to calculations [55]. At the same time, electron transfer from P_A^* to Φ_B in the B_B site in HM182L mutant RC of *Rb. sphaeroides* and in *C. aurantiacus* RC is possible if the LUMO energy of Φ_B is lower than that of P_A^*. The nuclear configuration in the state with the 895-nm emission

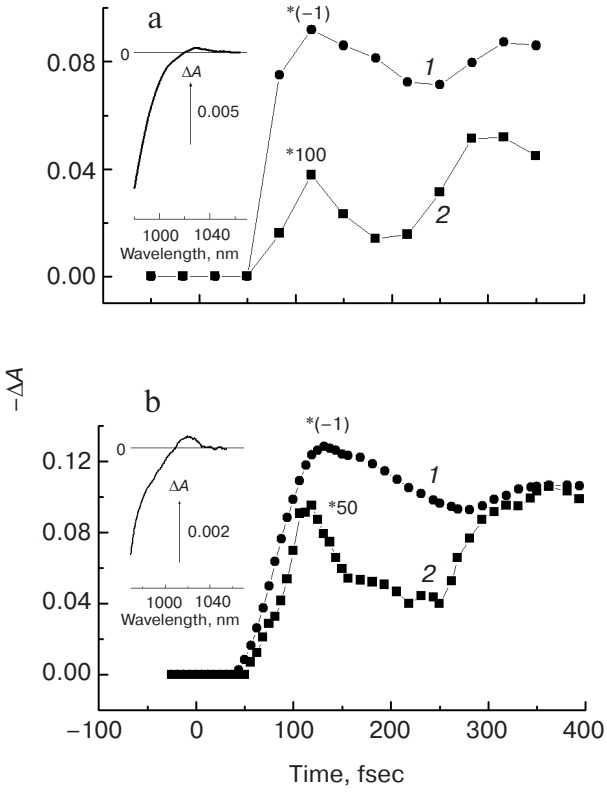

Fig. 5. Kinetics of ΔA of *C. aurantiacus* RC (a) and of mutant HM182L RC of *Rb. sphaeroides* (b) at 940 (*1*) and 1020-1028 nm (*2*) in the delay range of −100 to 400 fsec. In the insets, the characteristic ΔA spectra in the 990-1050 nm region are shown. The *C. aurantiacus* data are taken from [49], and mutant HM182L data are taken from [50]. RCs were excited by 20-fsec pulses at 870 nm at 90 K.

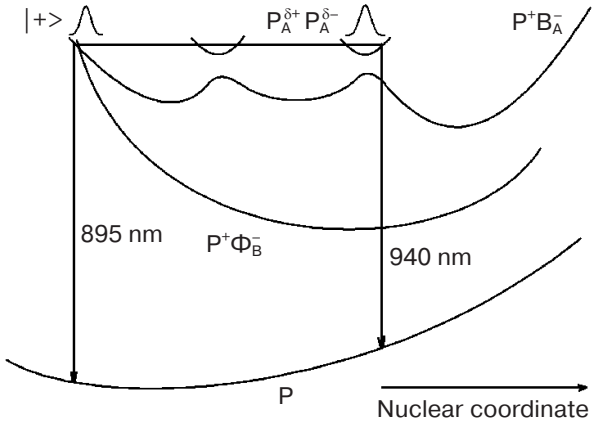

Fig. 6. Simplified scheme of the diabatic (phonon) potential energy surfaces of the ground ($\Phi_B PB_A H_A$) and locally excited ($\Phi_B P^* B_A H_A$) states as well as the charge separated states ($\Phi_B^- P^+ B_A H_A$ and $\Phi_B P^+ B_A^- H_A$). Strong electron coupling between P_A and P_B (~600 cm^{-1}) leads to the appearance of the two electronic states in P*: $|\pm> \equiv \sqrt{½}\{|P_A^* P_B> \pm |P_A P_B^*>\}$. The lower state |+> and the charge separated state $|P_A^{\delta+}P_B^{\delta-}>$ have different potential energy surfaces and can interact because of strong energy coupling. It is supposed that the emission from the surface of the |+> state occurs at ~895 nm, while from the surface of the $|P_A^{\delta+}P_B^{\delta-}>$ state is at ~935-940 nm due to the different displacements of the surfaces with respect to the ground state surface. The electron coupling between P* and B_A (~30 cm^{-1}) leads to the splitting of the two original surfaces (P* and $P^+B_A^-$) into the upper and lower surfaces. It is supposed that the surface of the $P_A^{\delta+}P_B^{\delta-}$ state intersects with the $P^+B_A^-$ surface in the bottom part of $P_A^{\delta+}P_B^{\delta-}$. The nuclear wave packet with high energy (~150 cm^{-1}) can reach the upper parts of the P^*B_A and $P^+B_A^-$ surfaces in the point of their intersection, which causes the appearance of P* stimulated emission at 940 nm and B_A^- absorption at 1020 nm with a subsequent reflection of the packet back to the P* surface or partial transition to the $P^+B_A^-$ surface. Electron transfer to Φ_B in RCs of *C. aurantiacus* and of HM182L *Rb. sphaeroides* mutant can occur from the surface of the |+> state.

seems to be optimal for such electron transfer. Femtosecond bleaching at 785 nm in HM182L mutant RC [50] and at 785 and 748 nm in *C. aurantiacus* RC (Fig. 2) proves this assumption. The nuclear wave packet moving on the |+> surface [5] with 140-160 cm^{-1} frequency can reach the $P_A^{\delta+}P_B^{\delta-}$ surface at the ~120-fsec delay. In this case, the fraction of the $P_A^{\delta+}P_B^{\delta-}$ state is much increased, which accelerates electron transfer to B_A. At the ~120-fsec delay the P* stimulated emission occurs at 940 nm and the B_A^- absorption band formation occurs at 1020-1028 nm (Fig. 5). A possibility of direct electron transfer from P_B^* to B_A cannot be excluded, though a connection of nuclear motion on the potential surface in the 940-nm emission area (Fig. 6) with the electron transfer from P* to B_A does not confirm it. The $P_A^{\delta+}P_B^{\delta-}$ state formation can be effective because the π-electron density of P* is mostly localized (0.74/0.26) in the P_B-half of the dimer [55]. Then the 940-nm emission can be related to exciplex formation [56, 57].

It is supposed that the oscillations with 130-150 cm^{-1} frequency in the kinetics of P* stimulated emission and of $P^+B_A^-$ product reflect the motion of P_B with respect to P_A in the area of overlapping of rings I of P_A and P_B [58]. One of the consequences of this motion might be the formation of a complex of excited molecules during the charge separation similar to the well-known excimer and exciplex of aromatic rings of excited dye molecule dimers in solution [56, 57]. One can assume that the same excited dimers are formed from two (B) Chl molecules in P870 (and perhaps in P700 of photosystem I of green plants) when ring I of P_B is shifted closest to ring I of P_A. Then the long-wavelength P* stimulated emission at 940 nm at 120-fsec delay can be explained by "dynamic" formation of the exciplex consisting of P_A and P_B. The fact of electron density shift from P* to B_A with the formation of the B_A^- absorption band at 1020 nm at the same delay strongly supports this suggestion. In the terms of the resonance electron–photon orbits in the conjugated π-electron systems, the formation of excimer and exciplex can be considered as an interference of the two monomer orbits in the dimer when they are close enough.

Thus, in the present work a conclusion is made about coherent electron transfer in B-branch of *C. aurantiacus* RC by comparing femtosecond spectroscopy data of *C. aurantiacus* RC and HM182L mutant RC of *Rb. sphaeroides* [50]. Unambiguous assignment of the 785-nm band in the HM182L mutant to the Q_y transition of the Φ_B molecule have helped us to conclude that the same Φ_B molecule in *C. aurantiacus* RC has the Q_y transition at 748 as well as at 785 nm. In RCs of HM182L mutant the coherent reversible electron transfer in the B-branch with $P^+\Phi_B^-$ state formation occurs immediately after femtosecond excitation. At this moment the nuclear wave packet is on the short-wavelength part of the P* potential surface that leads to the stimulated emission at 895 nm. Electron transfer to the A-branch with the formation of the $P^+B_A^-$ state develops later at the 120-fsec delay [50], when the wave packet moves to the opposite side of the P* potential surface and the P* emission is observed at 940 nm. The analysis of *C. aurantiacus* RC femtosecond kinetics at 785 and 748 nm shows that in this RC the Φ_B molecule is reversibly reduced by an electron from P* earlier than electron transfer from P* to B_A begins with further stabilization of the $P^+B_A^-$ state. Thus, the femtosecond reversible electron transfer between P* and BPheo molecule in the B_B site is a common feature of *C. aurantiacus* and HM182L mutant of *Rb. sphaeroides* RCs. In *C. aurantiacus* RC the reversible formation of the $P^+\Phi_B^-$ state occurs on the background of the unidirectional unambiguous electron transfer to the A-branch, which is confirmed by close-to-unity quantum yield of the primary charge separation [25, 26]. A different situation is observed in HM182L mutant RC, where the $P^+\Phi_B^-$ state is detected in the picosecond time domain by global analysis of ΔA spectra [34]. Perhaps a partial irreversible picosecond stabilization of the $P^+\Phi_B^-$ state formed right after excitation occurs in this RC. No data on such stabi-

lization are available at the present time [50]. However, the quantum yield of $P^+\Phi_B^-$ state formation in HM182L mutant RC is rather low (12% at 77 and 9 K [34]). In this RC, the absorption decrease at 785 nm at delays longer than 100 fsec is completely masked by interference with absorption changes of other processes [50].

This work was financed by grants from the Russian Academy of Sciences (Molecular and Cell Biology program), the Russian Foundation for Basic Research (grant No. 08-04-00888a), NWO (No. 047-009-008), INTAS (No. 00-0404**)**, and the Russian Federation Ministry of Education and Science.

REFERENCES

1. Deisenhofer, J., Epp, O., Miki, K., Huber, R., and Michel, H. (1984**)** *J. Mol. Biol.*, **180**, 385-398.
2. Allen, J. P., Feher, G., Yeates, T. O., Komiya, H., and Rees, D. C. (1987) *Proc. Natl. Acad. Sci. USA*, **84**, 5730-5734.
3. Kirmaier, C., and Holten, D. (1993) in *The Photosynthetic Reaction Center* (Deisenhofer, J., and Norris, J., eds.) Academic Press, San Diego, pp. 49-70.
4. Woodbury, N. W., and Allen, J. P. (1995) in *Anoxygenic Photosynthetic Bacteria* (Blankenship, R. E., Madigan, M. T., and Bauer, C. E., eds.) Kluwer Academic Publishers, Dordrecht, pp. 527-557.
5. Shuvalov, V. A., and Yakovlev, A. G. (2003) *FEBS Lett.*, **540**, 26-34.
6. Feick, R., Shiozawa, J. A., and Ertlmaier, A. (1995) in *Anoxygenic Photosynthetic Bacteria* (Blankenship, R. E., Madigan, M. T., and Bauer, C. E., eds.) Kluwer Academic Publishers, Dordrecht, Netherlands, pp. 699-708.
7. Bruce, B. D., Fuller, R. C., and Blankenship, R. E. (1982) *Proc. Natl. Acad. Sci. USA*, **79**, 6532-6536.
8. Kirmaier, C., Holten, D., Feick, R., and Blankenship, R. E. (1983) *FEBS Lett.*, **158**, 73-78.
9. Kirmaier, C., Blankenship, R. E., and Holten, D. (1986) *Biochim. Biophys. Acta*, **850**, 275-285.
10. Blankenship, R. E., Feick, R., Bruce, B. D., Kirmaier, C., Holten, D., and Fuller, R. C. (1983) *J. Cell. Biochem.*, **22**, 251-261.
11. Vasmel, H., and Amesz, J. (1983) *Biochim. Biophys. Acta*, **724**, 118-122.
12. Hale, M. B., Blankenship, R. E., and Fuller, R. C. (1983) *Biochim. Biophys. Acta*, **723**, 376-382.
13. Venturoli, G., Trotta, M., Feick, R., Melandri, B. A., and Zannoni, D. (1991) *Eur. J. Biochem.*, **202**, 625-634.
14. Feick, R., Ertlmaier, A., and Ermler, U. (1996) *FEBS Lett.*, **396**, 161-164.
15. Ovchinnikov, Yu. A., Abdulaev, N. G., Zolotarev, A. S., Shmuckler, B. E., Zargarov, A. A., Kutuzov, M. A., Telezhinskaya, I. N., and Levina, N. B. (1988) *FEBS Lett.*, **231**, 237-242.
16. Ovchinnikov, Yu. A., Abdulaev, N. G., Shmuckler, B. E., Zargarov, A. A., Kutuzov, M. A., Telezhinskaya, I. N., Levina, N. B., and Zolotarev, A. S. (1988) *FEBS Lett.*, **232**, 364-368.
17. Shiozawa, J. A., Lottspeich, F., Oesterhelt, D., and Feick, R. (1989) *Eur. J. Biochem.*, **180**, 75-84.
18. Vasmel, H., Meiburg, R. F., Kramer, H. J. M., de Vos, L. J., and Amesz, J. (1983) *Biochim. Biophys. Acta*, **724**, 333-339.
19. Parot, P., Delmas, N., Garcia, D., and Vermeglio, A. (1985) *Biochim. Biophys. Acta*, **809**, 137-140.
20. Shuvalov, V. A., Shkuropatov, A. Ya., Kulakova, S. M., Ismailov, M. A., and Shkuropatova, V. A. (1986) *Biochim. Biophys. Acta*, **849**, 337-346.
21. Vasmel, H., Amesz, J., and Hoff, A. J. (1986) *Biochim. Biophys. Acta*, **852**, 159-168.
22. Scherer, P. O. J., and Fischer, S. F. (1987) *Biochim. Biophys. Acta*, **891**, 157-164.
23. Becker, M., Nagarajan, V., Middendorf, D., Parson, W. W., Martin, J. E., and Blankenship, R. E. (1991) *Biochim. Biophys. Acta*, **1057**, 299-312.
24. Feick, R., Martin, J.-L., Breton, J., Volk, M., Scheidel, G., Langenbacher, T., Urbano, C., Ogrodnik, A., and Michel-Beyerle, M. E. (1990) in *Reaction Centers of Photosynthetic Bacteria* (Michel-Beyerle, M. E., ed.) Springer-Verlag, Berlin, pp. 181-188.
25. Volk, M., Scheidel, G., Ogrodnik, A., Feick, R., and Michel-Beyerle, M. E. (1991) *Biochim. Biophys. Acta*, **1058**, 217-224.
26. Wachtveitl, J., Huber, H., Feick, R., Rautter, J., Muh, F., and Lubitz, W. (1998) *Spectrochim. Acta*, Pt. A, **54**, 1231-1245.
27. Shuvalov, V. A., Vasmel, H., Amesz, J., and Duysens, L. N. M. (1986) *Biochim. Biophys. Acta*, **851**, 361-368.
28. Pierson, B. K., and Thornber, J. P. (1983) *Proc. Natl. Acad. Sci. USA*, **80**, 80-84.
29. Parson, W. W., Chu, Z.-T., and Warshel, A. (1990) *Biochim. Biophys. Acta*, **1017**, 251-272.
30. Gunner, M. R., Nicholls, A., and Honig, B. (1996) *J. Phys. Chem.*, **100**, 4277-4291.
31. Watanabe, T., and Kobayashi, M. (1991) in *Chlorophylls* (Scheer, H., ed.) CRC Press, Boca Raton, FL, pp. 287-315.
32. Fajer, J., Brune, D. C., Davis, M. S., Forman, A., and Spaulding, L. D. (1975) *Proc. Natl. Acad. Sci. USA*, **72**, 4956-4960.
33. Katilius, E., Turanchik, T., Lin, S., Taguchi, A. K. W., and Woodbury, N. W. (1999) *J. Phys. Chem. B*, **103**, 7386-7389.
34. Katilius, E., Katiliene, Z., Lin, S., Taguchi, A. K. W., and Woodbury, N. W. (2002) *J. Phys. Chem. B*, **106**, 1471-1475.
35. Schweitzer, G., Hucke, M., Griebenow, K., Muller, M. G., and Holzwarth, A. R. (1992) *Chem. Phys. Lett.*, **190**, 149-154.
36. Aumeier, W., Eberl, U., Ogrodnik, A., Volk, M., Scheidel, G., Feick, R., Plato, M., and Michel-Beyerle, M. E. (1990) in *Current Research in Photosynthesis* (Baltscheffsky, M., ed.) Vol. 1, Kluwer Academic Publishers, Dordrecht, Netherlands, pp. 133-136.
37. Vos, M. H., Lambry, J.-C., Robles, S. J., Youvan, D. C., Breton, J., and Martin, J.-L. (1991) *Proc. Natl. Acad. Sci. USA*, **88**, 8885-8889.
38. Vos, M. H., Rappaport, F., Lambry, J.-C., Breton, J., and Martin, J.-L. (1993) *Nature*, **363**, 320-325.
39. Vos, M. H., Jones, M. R., Hunter, C. N., Breton, J., Lambry, J.-C., and Martin, J.-L. (1994) *Biochemistry*, **33**, 6750-6757.
40. Vos, M. H., Jones, M. R., Breton, J., Lambry, J.-C., and Martin, J.-L. (1996) *Biochemistry*, **35**, 2687-2692.
41. Stanley, R. J., and Boxer, S. G. (1995) *J. Phys. Chem.*, **99**, 859-863.

42. Sporlein, S., Zinth, W., and Wachtveitl, J. (1998) *J. Phys. Chem. B*, **102**, 7492-7496.
43. Streltsov, A. M., Vulto, S. I. E., Shkuropatov, A. Ya., Hoff, A. J., Aartsma, T. J., and Shuvalov, V. A. (1998) *J. Phys. Chem. B*, **102**, 7293-7298.
44. Yakovlev, A. G., Shkuropatov, A. Ya., and Shuvalov, V. A. (2000) *FEBS Lett.*, **466**, 209-212.
45. Yakovlev, A. G., and Shuvalov, V. A. (2000) *J. Chin. Chem. Soc.*, **47**, 709-714.
46. Yakovlev, A. G., Shkuropatov, A. Ya., and Shuvalov, V. A. (2002) *Biochemistry*, **41**, 2667-2674.
47. Yakovlev, A. G., Shkuropatov, A. Ya., and Shuvalov, V. A. (2002) *Biochemistry*, **41**, 14019-14027.
48. Vos, M. H., Rischel, C., Jones, M. R., and Martin, J.-L. (2000) *Biochemistry*, **39**, 8353-8361.
49. Yakovlev, A. G., Vasilieva, L. G., Shkuropatov, A. Ya., Bolgarina, T. I., Shkuropatova, V. A., and Shuvalov, V. A. (2003) *J. Phys. Chem. A*, **107**, 8330-8338.
50. Yakovlev, A. G., Shkuropatova, T. A., Vasilieva, L. G., Shkuropatov, A. Ya., and Shuvalov, V. A. (2006) *Biochim. Biophys. Acta*, **1757**, 369-379.
51. Shiozawa, J. A., Lottspeich, F., Oesterhelt, D., and Feick, R. (1987) *Eur. J. Biochem.*, **167**, 595-600.
52. Blankenship, R. E., Trost, J. T., and Manchino, L. J. (1988) in *The Photosynthetic Bacterial Reaction Center: Structure and Dynamics* (Breton, J., and Vermeglio, A., eds.) Plenum Press, New York-London, pp. 119-127.
53. De Winter, A., and Boxer, S. G. (1999) *J. Phys. Chem.*, **103**, 8786-8789.
54. Ando, K., and Sumi, H. (1998) *J. Phys. Chem. B*, **102**, 10991-11000.
55. Plato, M., Lendzian, F., Lubitz, W., Trankle, E., and Mobius, K. (1988) in *The Photosynthetic Bacterial Reaction Center: Structure and Dynamics* (Breton, J., and Vermeglio, A., eds.) Plenum Press, New York-London, pp. 379-388.
56. Terenin, A. N. (1967) *Photonics of Dye Molecules* [in Russian], Nauka, Moscow.
57. Beens, H., and Weller, A. (1975) in *Organic Molecular Photophysics* (Birks, J. B., ed.) Vol. 11, John Willey & Sons, London, pp. 159-215.
58. Shuvalov, V. A. (2007) *Biochim. Biophys. Acta*, **1767**, 422-433.